Int. J. Electrochem. Sci., 16 **(2021)** Article ID: 21078, doi: 10.20964/2021.07.14

International Journal of
ELECTROCHEMICAL
SCIENCE
www.electrochemsci.org

Mini Review

Research Advance of Multi-anionic Compound Nanomaterials in Electrocatalytic Water Decomposition

Xin Liu[1,2], Lin Zhu[2], Keying Cui[1,2], Runyu Gao[2] ,Yan Liu[2], Jialin Xu[2], Haoran Ma[2], and Weimin Du[2,]*

[1] College of Chemistry, Zhengzhou University, Zhengzhou, Henan, 450001, China
[2] Henan Province Engineering Laboratory of Chemical Energy-saving Material Development and Application, College of Chemistry and Chemical Engineering, Anyang Normal University, Anyang, Henan, 455002, China,
[*]E-mail: dwmchem@163.com

Received: 1 March 2021 / *Accepted:* 7 April 2021 / *Published:* 31 May 2021

Due to the large surface area, lots of active sites and the better synergy, multi-anionic compound nanomaterials usually have the improved electrocatalytic activity and other special physicochemical properties. However, compared to the synthesis and catalytic application of multi-cation compound nanomaterials, the research on multi-anionic compound nanomaterials is lagged a lot, especially in the field of hydrogen production by electrolysis of water. Therefore, the recent research advance of multi-anionic compound nanomaterials are detailed reviewed in this paper, including: preparation methods, structural characteristics, electrocatalytic performance and internal mechanism. Some suggestions are made for the future development of multi-anion compound nanomaterials.

Keywords: Research advance; Multi-anionic; Nanomaterials; Electrocatalysis; Water decomposition.

1. INTRODUCTION

With global warming and water pollution problems becoming more serious, it is imminently to explore the clean, sustainable energy (e.g.: solar, wind, ocean and geothermal energy) for replacing fossil fuels with increasing scarcity and unfriendly environmental [1-3]. Yet, it is very hard to directly utilize these new types of energy in a controllable way [4]. Hydrogen is a promising carrier of new energy due to the high energy density of 120 MJ/kg and zero pollutant emissions [5]. Therefore, storing these new energy sources in the form of hydrogen will be an effective mean to solve the above problems. Although the hydrogen production by electrolysis of water is an efficient approach, it need the high-efficient catalyst to ensure the energy conversion efficiency [6-8]. At present, platinum-based metallic catalysts show the wonderful performance. But the expensive price limits the large-scale application [9-13]. Thus, it is very necessary for seeking the ideal catalysts with excellent catalytic performance, good stability

and cost-effective [14, 15].

Until now, many functional nanomaterials are used as the electro-catalysts for hydrogen production by electrolysis of water, e.g.: transition metallic compound [4]、single atom precious metal [16]、perovskite [17], and so on[18-22]. Among these, transition metallic compound nanomaterials have become the new generation of water-splitting catalysts due to their good conductivity, wide source and high availability. Although the catalytic application of transition metallic sulfides, selenides and phosphides have been devoted great efforts, the performance of these catalysts still need to be greatly improved compared to Pt [23-27]. Today, there are two strategies for enhancing the electrocatalytic properties: (1) Improving the dispersion and conductivity of catalyst supporter and exposing more activity edge sites. This method can obviously improve the catalytic performance of powder catalysts. But it also decreases the effect of self-supporting catalysts. (2) Tuning electronic structure by heteroatom doping, defect engineering, strain engineering, and interface engineering, etc. This electronic structure adjustment can build an electronic connection network, and reduce the transfer resistance in the catalytic process, thereby increasing the catalytic effect. Thus, tuning electronic structure based on the coexistence of different elements is regarded as the excellent strategy for achieving high-performance catalysts. Multi-element compound nanomaterials usually include multi-cation compound nanomaterials, multi-anion compound nanomaterials, and composite nanomaterials, etc. Among these, multi-anion compound nanomaterials can reduce the overlap of the metal *d* orbital, and result in a *d*-band center closer to the Fermi level. It will enhance the inherent conductivity, optimize the reaction path, and greatly improve the electro-catalytic properties [28]. However, compared to the rapid development of multi-cation compound nanomaterials, the catalytic research of multi-anion compound nanomaterials is lagged a lot. Until recently, some multi-anionic compound nanomaterials are obtained and applied in electrocatalytic field. For example: $Mo(S_{1-X}Se_X)_2$ nanoparticles need the overpotential of 161 mV vs. RHE (Reversible Hydrogen Electrode) at 10 mA cm^{-2} [29]. $Ni(S_{0.49}Se_{0.51})_2$ porous flake array need 113 mV vs. RHE overpotential at 10 mA cm^{-2} for hydrogen evolution reaction [30]. Cu_2Se-Cu_2O as OER catalyst need 465 mV vs. RHE overpotential at 10 mA cm^{-2} [31]. All of these results indicate that multi-anion compound nanomaterials are very promising as catalysts for electrolysis of water. Therefore, this review summaries the recent research advance of multi-anionic compound nanomaterials, including the synthesis, the application in electrocatalytic water decomposition, the challenges and the future outlook.

2. BASIC PRINCIPLES OF WATER DECOMPOSITION

2.1. Hydrogen evolution reaction (HER)

Water decomposition can produce hydrogen and oxygen under the action of direct current [19, 32, 33]. Hydrogen is produced on the cathode, which is a two-electron transfer process. The reaction of producing hydrogen could be described in the following steps [34-36].

(1) Volmer reaction:

$$\mathbf{H^+ + M + e^- \rightarrow MH_{ads}} \quad \text{(in acid)}$$

$$\mathbf{H_2O + M + e^- \rightarrow MH_{ads} + OH^-} \quad \text{(in alkali)}$$

(2) Heyrovsky reaction:

$\mathbf{MH_{ads} + H^+ + e^- \rightarrow MH_{ads} + H_2}$ (in acid)

$\mathbf{MH_{ads} + H_2O + e^- \rightarrow M + H_2 + OH^-}$ (in alkali)

(3) Tafel reaction: $\mathbf{2MH_{ads} \rightarrow 2M + H_2}$

M is the catalytic sites, H_{ads} is adsorbed hydrogen. Hydrogen adsorption is the key factor in HER [37]. These reaction mechanism are frequently combined to the Tafel formula. The Tafel formula is as follows: $\boldsymbol{\eta = a + b \log j}$ [38]. Here η (mV) is overpotential; a and b ($mVdec^{-1}$) are Tafel constant that are related to electrode material temperature, surface shape, solution and so on; J ($mA\ cm^{-2}$) is the exchange current density with positive value. When $30 < b < 40$ mV dec^{-1}, HER may go through Volmer-Tafel reaction process； When $40 < b < 120$ mV dec^{-1}, HER will undergo the Volmer-Heyrovsky reaction. Hence, HER can be class as Volmer-Heyrovsky process and Volmer-Tafel process [39]. Different materials have different speed-limit steps, which will result in different b values. The smaller the b value, the faster the electron transfer speed and the better the catalytic effect [40]. Besides, low resistance (Rs), high activity and low Gibbs free energy are also conducive to the HER activity of electrode materials.

2.2 Oxygen evolution reaction (OER)

Compared to HER, OER is a four-electron-proton coupling reaction. It requires a higher energy barrier, resulting in a high demand for overpotential. Therefore, the overpotential of OER is higher than the theoretical decomposition voltage of water (1.23V). There are many references explaining the reaction mechanism. Although oxygen electrode produce has not an utter verdict, but some mechanism has been common given in neutral or alkaline solution [41]:

$\mathbf{M + OH^- \rightarrow MOH + e^-}$

$\mathbf{MOH + OH^- \rightarrow MO + H_2O + e^-}$

$\mathbf{MO + OH^- \rightarrow MOOH + e^-}$

$\mathbf{MOOH + OH^- \rightarrow M + O_2 + H_2O + e^-}$

Also that has been provided in acid solution [37]:

$\mathbf{M + H_2O \rightarrow MOH + H^+ + e^-}$

$\mathbf{MOH \rightarrow MO + H^+ + e^-}$

$\mathbf{MO + H_2O \rightarrow MOOH + H^+ + e^-}$

$\mathbf{MOOH \rightarrow M + O_2 + H^+ + e^-}$

OER involves many reaction intermediates, and the energy barrier of each step of the reaction together make up a complex reaction kinetics and high overpotential [42].

2.3 Overall water splitting

The overpotential of overall water splitting can be described as:

$$\boldsymbol{\eta = 1.23 + \eta_a + \eta_b + \eta_{other}}$$

η_a is overpotential of OER, η_b is overpotential of HER, η_{other} is the overpotential from other factor

(solution resistance, electrode resistance and contact resistance). Comprehensive considering the HER and OER in electrolyzed water, the main factors for catalytic performance are overpotential, Tafel slope, stability, and so forth [43-44]. To get high efficiency catalytic performance, the selected electrocatalytic materials usually have the following traits: unique structure, high surface area, and low resistance, and so on [45].

3. SYNTHETIC METHODS OF MULTI-ANIONIC COMPOUND NANOMATERIALS

Multi-anionic compound nanomaterials are a kind of promising catalysts for electrocatalysis. Hence, some multi-anionic compound nanomaterials with different composition and/or morphologies were prepared, e.g., $Mo(S_{1-x}Se_x)_2$[29], $NiS_{2(1-x)}Se_{2x}$[46], $Co(S_{0.73}Se_{0.27})_2$[47], $WS_{2(1-x)}Se_{2x}$ [48], Co-Mo-O-S [4], Cu_2Se-Cu_2O [31], Ni-Co-S-Se[49], CoFe-Se-P[50], $CoP_{2x}Se_{2(1-x)}$ [33], O-$CoSe_2$-HNT[51], etc. The following several synthetic methods are often used during the synthetic process.

3.1. Hydrothermal synthesis

Hydrothermal synthesis usually bases on the liquid-phase chemical reaction. The reaction temperature is about 100-1000 ºC and the pressure is from1 Mpa to 1 Gpa. The mechanism of homogeneous or heterogeneous nucleation in hydrothermal reaction is very different from that of solid phase reaction. Hence, some new nanomaterials with unique structure and properties can be achieved.

1T/2H $Mo(S_{1-X}Se_{1-X})_2$ nanoparticles have been achieved via a hydrothermal method. The coexistence of S and Se elements can decrease the reaction energy and 1T phase could enhance the conductivity. Thus, 1T/2H Mo $(S_{1-X}Se_{1-X})_2$ nanoparticles exhibit excellent electrocatalytic performance [29]. $NiS_{2(1-x)}Se_{2x}$ hollow porous spheres are achieved through a hydrothermal Ostwald ripening process (See Figure 1). By adjusting the degree of selenization and controlling the selenium-sulfur ratio, the nickel adjustable electronic structure is realized. Therefore, these $NiS_{2(1-x)}Se_{2x}$ hollow spheres have the improved catalytic activity [46].

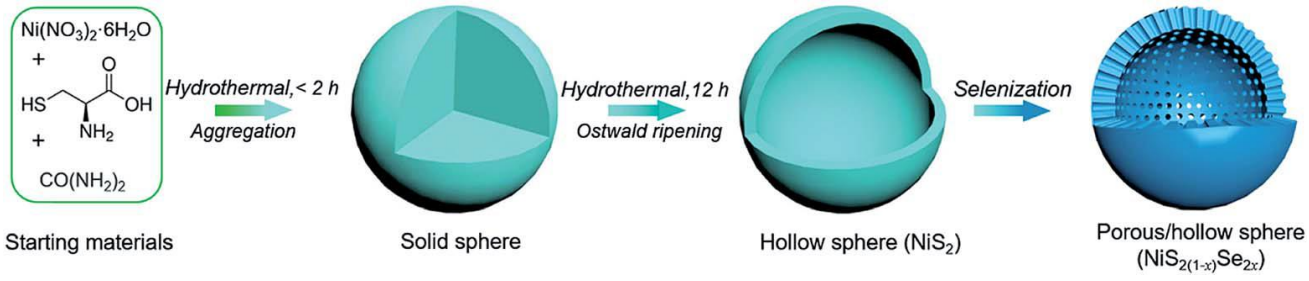

Figure 1. Schematic illustration of the formation of $NiS_{2(1-x)}Se_{2x}$ hierarchical hollow spheres (Reprinted with permission from *Journal of Materials Chemistry* A, 7 (**2019**) 16793. Copyright (2019) The Royal Society of Chemistry.)

Ternary $Ni(S_{0.49}Se_{0.51})_2$ porous nanosheet array is grown on the carbon fiber cloth (CFC) by chemical hydrothermal method. $Ni(S_{0.49}Se_{0.51})_2$ takes on the flake-like shape whose surface are very

rough due to the existence of particles and pores [30]. With carbon fiber paper (CFP) as the substrate, $Co(OH)(CO_3)_{0.5}$ nanowires (NWs) is successfully synthesized by hydrothermal method, then converted into $Co(S_xSe_{1-x})_2$ NWs with controllable composition. By adjusting the components, $Co(S_{0.73}Se_{0.27})_2$ NWs exhibit the optimal electrocatalytic activity towards HER [47]. Compared to other methods, hydrothermal method is the most commonly used method for obtaining multi-anionic compounds or composite materials.

3.2. Solvothermal synthesis

Compared with hydrothermal method, the major different of solvothermal method is the non-aquatic solvent. Interestingly, the solvothermal synthesis may produce some nanomaterials with unusual morphologies. Some distinctive multi-anionic compound nanomaterials have been obtained via solvothermal synthesis. The synthesized S-(NiCo)Se nanostructures have cubic $NiCo_2S_4$ and $NiSe_2$ phase. The electrochemical performance of S(NiCo)Se are superior to (NiCo)Se when S and Se can be uniform distribution [52]. Xu et al successfully prepared porous $MoS_2/MoSe_2$ nanostructure supported by graphene via a simple mixed solvothermal method (See Figure 2). The targeted products have the highly conductive graphitization network. This hybrid three-dimensional structure promotes the formation of two-dimensional nanosheets, exposes the active center and improves the electrical transfer between the catalyst and the electrode [53].

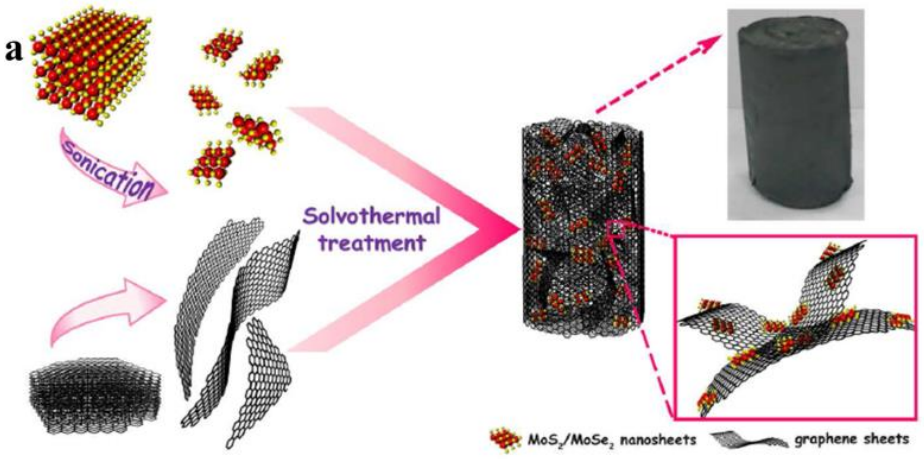

Figure 2. Schematic process of $MoS_2/MoSe_2$-graphene hybrid aerogel (Reprinted with permission from *Journal of Materials Chemistry A*, 3 (**2015**) 16337. Copyright (2015) The Royal Society of Chemistry.)

3.3. Chemical vapor deposition (CVD)

CVD is a synthetic method that utilizes the interface reaction of gaseous or vaporous substances to generate solid deposit. CVD usually includes the following three stages: the reaction gas diffuses to the substrate; the reaction gas adsorbs the substrate; and the chemical reaction occurs on the substrate surface to form solid deposit. The gas by-products are taken away from the substrate surface. Currently,

CVD has been widely applied to the preparation of various compounds. Zhang et al synthesized a new ternary electrocatalyst MoSxCly, which is an amorphous thin film grown on graphene [54]. Xu et al designed $WS_{2(1-X)}Se_{2X}$ nanotubes on the flexible carbon fibers(CFs) via CVD [48].

3.4. Electrochemical precipitations (EP)

Electrochemical deposition (EP) refers to a technique in which current flows in the electrolyte solution through the migration of anion and cation under the influence of an external electric field. Redox reactions of electron gain and loss occur on the electrode to form a coating film. Generally, EP can be divided into anode electro-deposition method (AEM) and cathode electro-deposition method (CEM). Compared to AEM, CEM is more widely used because the thickness of CEM film is more convenient to control. Chen et al grew Cu_2Se/Cu_2O nanoparticles on Ti foil by CEM method [31]. Jia et al fabricated n-p-Si/NiS_XO_y with a micro-pyramid structure via integrating an amorphous NiS_XO_y film and a Titanium-protected n^+p-Si. The unique structure and amorphous NiS_XO_y film achieve high HER electrocatalytic activity[55].

3.5. Self-template method

During the synthetic process of self-template, micro/nano scale “template” is firstly synthesized and then converted into a mesoporous or hollow structure. Unlike traditional template, this “self-template” can not only act as a supporting framework, but also directly participate in the shell formation process. The template material is directly converted into the targeted products with no need to remove. Up to date, the self-template method has made great progress in the preparation of multi-anionic compound nanomaterials with different morphologies. Jia et al synthesized the oxygen-modified nanotubes (O-$CoSe_2$-HNT) with a particle size of 300 nm and a uniform hierarchical distribution [51]. Co-Se-S-O ($CoSeS_{2-x}$@$Co(OH)_2$) nanotubes are obtained by selenizing and vulcanizing the Co(OH)F precursor in different solvent. It is of great significance for the preparation of $CoSe_XS_{2-X}$(Co-Se-S-O) nanotubes. As far as we knew, Co-Se-S-O is the first quaternary nanotube array, which unexpectedly improves the surface area and electrical conductivity [56].

4. ELECTROCHEMICAL CATALYSIS OF MULTI-ANIONIC COMPOUND NANOMATERIALS

The applications of multi-anionic compound nanomaterials are chiefly in the following three aspects: HER, OER, and overall water splitting [57-59].

4.1. Hydrogen evolution reaction (HER)

Hydrogen with zero pollution emissions and high energy density is an important substitute for traditional fossil fuels [42]. Electrochemical water decomposition has been known as the promising

method to product hydrogen.

Selenium-doped MoS_2 (Se-MoS_2) heterogeneous catalysts have been fabricated with $CoSe_2$ nanowires as the precursor. Compared to other non-noble electrocatalysts, the overpotential at 10 mA cm^{-2} of the heterogeneous catalyst (Se-MoS_2/$CoSe_2$) is very small, only 30 mV. The outstanding electrocatalytic activity can be attributed to a lot of active edges sites, high conductivity, high surface area, and the chemical bonding interface between $CoSe_2$ carrier and Se-MoS_2 kernel [57]. Zhou et al prepared the three-dimensional $MoS_{2(1-X)}Se_{2X}$ catalyst by growing vertically ordered layers on the porous $NiSe_2$ foam. The lower Tafel slope (42.1 mV dec^{-1}), the larger exchange current density (about 300 mA cm^{-2}), and the smaller overpotential (89 mV) fully prove the corresponding excellent HER performance. Furthermore, $MoS_{2(1-X)}Se_{2X}$ catalyst has stable performance for a long time (>16h) at a given potential (-121 mV) without significant degradation. Quantum mechanics calculations at the density functional theory (DFT) level were performed to calculate the binding free energies of hydrogen (ΔG_H^*) adsorbed on the Mo atom. Results indicate that ΔG_H^* for hydrogen adsorbed on $MoS_{2(1-x)}Se_{2x}$/$NiSe_2$ (100) and $MoS_{2(1-x)}Se_{2x}$/$NiSe_2$ (110) is much lower than those for MoS_2/MoS_2 and $MoS_{2(1-x)}Se_{2x}$/$MoS_{2(1-x)}Se_{2x}$ (See Figure 3). It makes $MoS_{2(1-x)}Se_{2x}$/$NiSe_2$ hybrid catalysts more active in the HER process [60]. Similar results also present in other works [61].

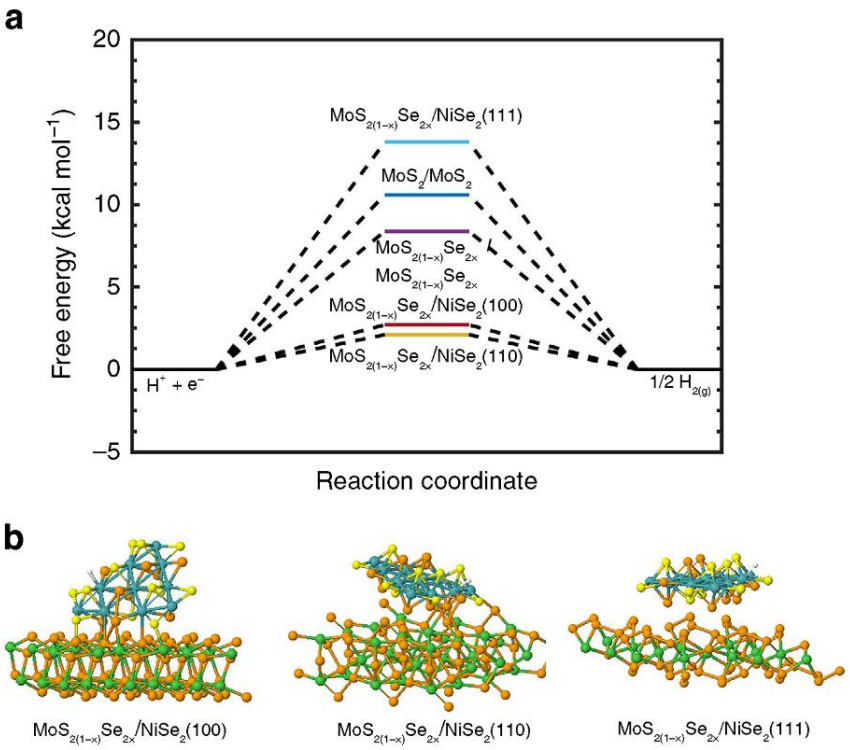

Figure 3. Density functional theory calculations. (a) Calculated adsorption free energy diagram for hydrogen (H*) adsorption at the equilibrium potential for $MoS_{2(1-x)}Se_{2x}$/$NiSe_2$ hybrid, binary MoS_2 and ternary $MoS_{2(1-x)}Se_{2x}$ catalysts. (b) Intermediate structures of hydrogen bound $MoS_{2(1-x)}Se_{2x}$ /$NiSe_2$ (100), $MoS_{2(1-x)}Se_{2x}$/$NiSe_2$ (110) and $MoS_{2(1-x)}Se_{2x}$ /$NiSe_2$ (111). (Reprinted with permission from *Nature Communications*, 7 (**2016**) 127651. Copyright (2016) Springer Nature.)

Wang et al prepared ternary $Co(S_XSe_{1-X})_2$ nanowires (NWs) by changing the molar ratio of S/Se.

$Co(S_{0.73}Se_{0.27})_2$ NWs can realize the low overpotential of 157 mV at100 mV/cm^2 in a 0.5 M H_2SO_4 solution, displaying the optimal and stable HER electrocatalytic activity. Furthermore, even after 20 h or 5000 cycles of continuous electrolysis in acidic electrolyte, good catalytic activity can still be maintained. DFT calculation results show that this excellent catalytic performance is attributed to the decrease of kinetic energy barrier, the large surface area and rapid electrolyte diffusion channels formed by the nano-sized electroactive matrix arranged [47].

Ultra-thin $MoS_{2(1-X)}Se_{2X}$ alloy nanoflakes with adjustable overall chemical composition are successfully prepared, which can effectively modify the *d*-band electronic structure of Mo by changing the ratio of S to Se. In the electrocatalytic reaction, the subtle modification of *d*-band can greatly improve the electrochemical activity of $MoS_{2(1-X)}Se_{2X}$ nanoflakes [62]. Compared with NiS_2 and $NiSe_2$, the porous $Ni(S_{0.49}Se_{0.51})_2$ sheets have excellent performance and good sustainability. It can drive a current density of 10 mA/cm^2 for HER at only 113 mV. It is attributed to the interaction of S and Se atoms, large specific surface area, more active centers, and superior conductivity [30].

In summary, multi-anionic compound nanomaterials are the excellent electrochemical catalysts for hydrogen evolution reaction. The corresponding lattice distortion can reduce the overlap of the metal *d* orbital, resulting in the *d*-band center closer to the Fermi level, increasing the inherent electronic conductivity, optimizing the reaction path, and greatly improving the electro-catalytic performance.

4.2. Oxygen evolution reaction (OER)

In the research field of electrochemical water splitting and metal-air batteries, OER is the important half reaction for energy conversion and storage [63-65]. Currently, most electrochemical catalysts are mainly concentrate on precious metals, such as RuO_2 or IrO_2 [66]. As a result, oxygen evolution reaction (OER) process is very inert, easily polarized and costly, which largely hinders their practical large-scale application. Hence, it is urge to develop economic non-precious metallic catalysts.

Chen et al prepared Cu_2Se-Cu_2O hybrid materials with high electrochemical activity for OER. Surface of Cu_2Se-Cu_2O catalyst is covered with CuO protective layer which can effectively curb the Cu_2Se-Cu_2O further oxidation, promote the catalytic oxidation of water. Thus, the overpotential is as low as 465 mV at 10 $mAcm^{-2}$and the Tafel slop is 140 mV dec^{-1}. The better catalytic performance of Cu_2Se-Cu_2O catalysts are from the big active specific surface area and rapidly electron transport [31]. Jia et al produced O-$CoSe_2$-HNT (HNT: nanotubes) with a diameter of 300 nm and a uniformly distributed hierarchical structure. O-$CuSe_2$-HNT needs only an overpotential of 252 mV, which is much lower than that of IrO_2 and RuO_2 (330 mV and 280 mV). Its excellent electrochemical performance is inseparable from oxygen modification on the catalyst surface [51].

Ni(Fe)OxHy nanosheets are grown on the stainless steel mesh without any polymer binder. Ni(Fe)OxHy nanosheet electrode has excellent OER properties, i.e.: low overpotential, small Tafel slope and long-time durability in alkaline electrolyte. These excellent performance benefits from the 3D architecture with highly exposed surface and the closed contact between the active species and conductive substrate. This makes Ni(Fe)OxHy nanosheet to be one of the most promising OER electrode [67]. Binary NiSe and CoSe, ternary Ni-Co-Se and even quaternary Ni-Co-S-Se are developed. Among

them, $Ni_{0.25}Co_{0.65}S_{0.4}Se_{0.6}$ has the optimal OER performance. At 350 mV overpotential, the turnover frequency is measured as 24.84×10^{-3} S^{-1}, which is 7 orders higher than that of binary CoSe [49].

In short, the interface control strategy based on the coexistence of multiple anions can effectively improve the OER activity and other physicochemical properties. Therefore, multi-anionic compound nanomaterials are the promising electrocatalysts for OER due to the high specific surface area, lots of active sites and better synergy.

4.3. Overall water splitting

It is the core of overall water decomposition hydrolysis to find out the low cost and rich catalysts [68, 69]. For a long time in the past, people always studied the HER and OER catalysts which mainly focused on transition metallic compounds in the field of non-precious metals [70]. However, in the actual production process, water needs to be electrolyzed for hydrogen production in the same electrolyte. Thus, it is imperative to design and synthesize the bifunctional water-splitting catalyst. At present, nanomaterials of multianionic compounds are the promising ones.

Peapod‐like $Co(S_xSe_{1-x})_2$ nanoparticles encapsulated in carbon fibers were obtained by coating carbon fiber and an adjustable sulfuration/selenylation process with $Co(Co_3)_{0.5}(OH)_{0.11}H_2O$ nanowires as precursors. Due to the increase exposure of $Co(S_xSe_{1-x})_2$ active center, unique structure, and the excellent electron transport ability, $Co(S_{0.71}Se_{0.29})_2$ has the excellent HER performance and $Co(S_{0.22}Se_{0.78})_2$ has the best OER performance. With $Co(S_{0.71}Se_{0.29})_2$ and $Co(S_{0.22}Se_{0.78})_2$ as the pair electrodes, the current density for water-splitting can achieve 10 mA cm^{-2} at a potential of 1.63 V. In addition, the composites displayed a durable whole water splitting activity[71]. $NiS_{2(1-x)}Se_{2x}$ hollow/porous spheres was synthesized by a facile hydrothermal and then selenization strategy which is directly used in electrocatalytic water decomposition. $Ni(S_{0.5}Se_{0.5})_2$ has a high hydrogen evolution, oxygen evolution active and good stability. When applied as a bifunctional catalyst in neutral conditions, $Ni(S_{0.5}Se_{0.5})_2$ hollow/porous spheres can drive 10 mA cm^{-2} at a cell voltage of merely 1.87 V [46].

New mesporous CoFe-Se-P electrocatalysts are constructed based on a hollow cobalt-iron Prussian blue analog (CoFe-PBA). This catalyst has high-efficiency and long-term bifunctional catalytic performance due to the strong interaction between Co, Fe, Se and P. It can be used not only in HER, but also in OER. In a two-electrode water splitting system based on mesporous CoFe-Se-P, the cell voltage only need 1.59 V, demonstrating the excellent bifunctional activities and the better stabilization [50]. Ternary nanoporous $Cu_2O_XS_{1-X}$ has been grown on Cu foam. In order to probe the applied value, two-electrode catalytic device based on $Cu_2O_xS_{1-x}$ is constructed. The linear sweep voltammogram in 1.0 mol dm^{-3} KOH solution was recorded. At 10 or 20 mA cm^{-2}, the working potential is 1.56 V or 1.80 V which is lower than that of Pt/C and IrO_2 catalyst. This demonstrates $Cu_2O_XS_{1-X}$/Cu is a good catalyst for total water decomposition [72].

4. RESULTS AND PROSPECTS

All in all, multi-anionic compound nanomaterials have a wide range of application in the field of

electrochemical catalysis. The morphologies and structures can be adjusted by different elements and different production methods. The electrocatalytic performance can be improved by reasonably design the composition and/or introduce different anions. Despite of these, there are still some shortcomings in order to be further applied in the field of electrocatalyst. In the future, multi-anionic compound nanomaterials can be further explored in the following aspects：(1) Introducing more anions to design and synthesize novel multi-element compound nanomaterials with excellent electrocatalytic properties; (2) Design new configurations and structures based on the coupling of different catalysts; (3) Reasonably introduce the external factors of the electrolyzed water system, such as magnetic field, etc.

ACKNOWLEDGMENTS
This work was supported by the Grants from the from the Natural Science Foundation of Henan Province (212300410324), Basic Research Special of Key Scientific Research Project Plan in the Universities of Henan Province (20ZX007) and the Science and Technology Research Project of Henan Province (212102210037).

References

1. J.Cao, Y. Feng, B. Liu, and H. Li, *Science China Materials*, 61 (2018) 686.
2. Y. Cheng, X. Xiao, K. Pan, and H. Pang, *Chemical Engineering Journal*, 380 (2020) 122565.
3. E. López-Fernández, J. Gil-Rostra, J.P. Espinós, A.R. González-Elipe, A. de Lucas Consuegra, and F. Yubero, *ACS Catalysis*, 10 (2020) 6159.
4. X. Mao, Y. Zou, J. Liang, C. Xiang, H. Chu, E. Yan, H. Zhang, F. Xu, X. Hu, and L. Sun, *Ceramics International*, 46 (2020) 1448.
5. T. Shinagawa, and K. Takanabe, *Chemsuschem*, 10 (2017) 1318.
6. Y. Li, X. Tan, R.K. Hocking, X. Bo, H. Ren, B. Johannessen, S.C. Smith, and C. Zhao, *Nature Communications*, 11 (2020) 2720.
7. X. Yin, L. Yang, and Q. Gao, *Nanoscale*, 12 (2020) 15944.
8. H. Kumar, B. Bharti, S. Aslam, R.U.R. Sagar, K. Wang, L. Gan, P. Hua, X. Zeng, and Y. Su, *International Journal Of Energy Research*, 44 (2020) 7846.
9. P. Wang, R. Qin, P. Ji, Z. Pu, J. Zhu, C. Lin, Y. Zhao, H. Tang, W. Li, and S. Mu, *Small*, 16 (2020) 2001642.
10. Y.R. Zheng, P. Wu, M.R. Gao, X.L. Zhang, F.Y. Gao, H.X. Ju, R. Wu, Q. Gao, R. You, W.X. Huang, S.J. Liu, S.W. Hu, J. Zhu, Z. Li, and S.H. Yu, *Nature Communications*, 9 (2018) 2533.
11. G.M. Kumar, P. Ilanchezhiyan, H.D. Cho, D.J. Lee, D.Y. Kim, and T.W. Kang, *International Journal Of Energy Research*, 44 (2019) 811.
12. Z.P. Xiang, H.Q. Deng, P. Peljo, Z.Y. Fu, S.L. Wang, D. Mandler, G.Q. Sun, and Z.X. Liang, *Angewandte Chemie International Edition*, 57 (2018) 3464.
13. S. Ye, F. Luo, Q. Zhang, P. Zhang, T. Xu, Q. Wang, D. He, L. Guo, Y. Zhang, C. He, X. Ouyang, M. Gu, J. Liu, and X. Sun, *Energy & Environmental Science*, 12 (2019) 1000.
14. A.I. Inamdar, H.S. Chavan, B. Hou, C.H. Lee, S.U. Lee, S. Cha, H. Kim, and H. Im, *Small*, 16 (2020) 1905884.
15. X. Cui, Y. Cui, M. Chen, R. Xiong, Y. Huang, and X. Liu, *ACS Applied Materials & Interfaces*, 12 (2020) 30905.
16. Y. Yao, S. Hu, W. Chen, Z.-Q. Huang, W. Wei, T. Yao, R. Liu, K. Zang, X. Wang, G. Wu, W. Yuan, T. Yuan, B. Zhu, W. Liu, Z. Li, D. He, Z. Xue, Y. Wang, X. Zheng, J. Dong, C.-R. Chang, Y. Chen, X. Hong, J. Luo, S. Wei, W.-X. Li, P. Strasser, Y. Wu, and Y. Li, *Nature Catalysis*, 2 (2019) 304.

17. X. Li, H. Wang, Z. Cui, Y. Li, S. Xin, J. Zhou, Y. Long, C. Jin, and J.B. Goodenough, *Science Advances*, 5 (2019) 6262.
18. Y. Du, M. Zhang, Z. Wang, Y. Liu, Y. Liu, Y. Geng, and L. Wang, *Journal of Materials Chemistry* A, 7 (2019) 8602.
19. F. Yu, H. Zhou, Y. Huang, J. Sun, F. Qin, J. Bao, W.A. Goddard, 3rd, S. Chen, and Z. Ren, *Nature Communications*, 9 (2018) 2551.
20. J. Wang, J. Kim, S. Choi, H. Wang, and J. Lim, *Small Methods*, 4 (2020) 2000621.
21. Y. Kumaran, T. Maiyalagan, and S.C. Yi, *International Journal Of Energy Research*, 44 (2020) 1.
22. A.P. Murthy, J. Madhavan, and K. Murugan, *Journal Of Power Sources*, 398 (2018) 9.
23. T. Zhang, M.Y. Wu, D.Y. Yan, J. Mao, H. Liu, W.B. Hu, X.W. Du, T. Ling, and S.Z. Qiao, *Nano Energy*, 43 (2018) 103.
24. X. Zhong, J. Tang, J. Wang, M. Shao, J. Chai, S. Wang, M. Yang, Y. Yang, N. Wang, S. Wang, B. Xu, and H. Pan, *Electrochimica Acta*, 269 (2018) 55.
25. P. Liu, J. Li, Y. Lu, and B. Xiang, *International Journal Of Hydrogen Energy*, 43 (2018) 72.
26. K. Wang, Q. Chen, Y. Hu, W. Wei, S. Wang, Q. Shen, and P. Qu, *Small*, 14 (2018) 1802132.
27. Y.Z. Tian, Zhonghui， Miao, Yuqing, *Electrochemical Society*, 163 (2016) 625.
28. Y. Wang, X. Li, M. Zhang, Y. Zhou, D. Rao, C. Zhong, J. Zhang, X. Han, W. Hu, Y. Zhang, K. Zaghib, Y. Wang, and Y. Deng, *Advanced Materials*, 32 (2020) 2000231.
29. Z. Lin, B. Lin, Z. Wang, S. Chen, C. Wang, M. Dong, Q. Gao, Q. Shao, T. Ding, H. Liu, S. Wu, and Z. Guo, *ChemCatChem*, 11 (2019) 2217.
30. B. Xu, Z. Chen, H. Zhang, Y. Sun, and C. Li, *International Journal Of Hydrogen Energy*, 42 (2017) 30119.
31. H. Chen, Y. Gao, L. Ye, Y. Yao, X. Chen, Y. Wei, and L. Sun, *Chemical Communications*, 54 (2018) 4979.
32. H.A. Younus, Y. Zhang, M. Vandichel, N. Ahmad, K. Laasonen, F. Verpoort, C. Zhang, and S. Zhang, *Chemsuschem*, 13 (2020) 5088.
33. T. Tang, W.J. Jiang, S. Niu, N. Liu, H. Luo, Y.Y. Chen, S.F. Jin, F. Gao, L.J. Wan, and J.S. Hu, *Journal Of The American Chemical Society*, 139 (2017) 8320.
34. D. Lu, X. Ren, L. Ren, W. Xue, S. Liu, Y. Liu, Q. Chen, X. Qi, and J. Zhong, *ACS Applied Energy Materials*, 3 (2019) 3212.
35. Y. Shi, and B. Zhang, *Chemistry - An Asian Journal*, 45 (2016) 1781.
36. X. Zou, and Y. Zhang, *Chemical Society Reviews*, 44 (2015) 5148.
37. Q. Wang, C.Q. Xu, W. Liu, S.F. Hung, H. Bin Yang, J. Gao, W. Cai, H.M. Chen, J. Li, and B. Liu, *Nature Communications*, 11 (2020) 4246.
38. H. Vrubel, T. Moehl, M. Graetzel, and X. Hu, *Chemical Communications*, 49 (2013) 8985.
39. Masurkar, Nirul, Thangavel, Naresh, Kumar, Arava, Leela, Mohana, and Reddy, *ACS Applied Materials & Interfaces*, 10 (2018) 27771.
40. W. Cui, N. Cheng, Q. Liu, C. Ge, A.M. Asiri, and X. Sun, *ACS Catalysis* , 4 (2014) 2658.
41. N.T. Suen, S.F. Hung, Q. Quan, N. Zhang, Y.J. Xu, and H.M. Chen, *Chemical Society Reviews*, 46 (2017) 337.
42. S. Hu, S. Wang, C. Feng, H. Wu, J. Zhang, and H. Mei, *ACS Sustainable Chemistry & Engineering*, 8 (2020) 7414.
43. T. Kosmala, H. Coy Diaz, H.-P. Komsa, Y. Ma, A.V. Krasheninnikov, M. Batzill, and S. Agnoli, *Advanced Energy Materials*, 8 (2018) 1800031.
44. J. Bao, J. Wang, Y. Zhou, Y. Hu, Z. Zhang, T. Li, Y. Xue, C. Guo, and Y. Zhang, *Catalysis Science & Technology*, 9 (2019) 4961.
45. J. Bao, W. Liu, Y. Zhou, T. Li, Y. Wang, S. Liang, Y. Xue, C. Guo, Y. Zhang, and Y. Hu, *ACS Applied Materials & Interfaces*, 12 (2020) 2243.
46. L. Zeng, K. Sun, Y. Chen, Z. Liu, Y. Chen, Y. Pan, R. Zhao, Y. Liu, and C. Liu, *Journal of Materials Chemistry* A, 7 (2019) 16793.

47. K. Wang, C. Zhou, D. Xi, Z. Shi, C. He, H. Xia, G. Liu, and G. Qiao, *Nano Energy*, 18 (2015) 1.
48. K. Xu, F. Wang, Z. Wang, X. Zhan, Q. Wang, Z. Cheng, M. Safdar, and J. He, *Acs Nano*, 8 (2014) 8468.
49. M. Wang, Z. Dang, M. Prato, D.V. Shinde, L. De Trizio, and L. Manna, *ACS Applied Nano Materials*, 1 (2018) 5753.
50. L. He, B. Cui, B. Hu, J. Liu, K. Tian, M. Wang, Y. Song, S. Fang, Z. Zhang, and Q. Jia, *ACS Applied Energy Materials*, 1 (2018) 3915.
51. B. Jia, Z. Xue, Q. Liu, Q. Liu, K. Liu, M. Liu, T.-S. Chan, Y. Li, Z. Li, C.-Y. Su, and G. Li, *Journal of Materials Chemistry* A, 7 (2019) 15073.
52. J. Kim, R. Tabassian, V.H. Nguyen, S. Umrao, and I.K. Oh, *ACS Applied Materials & Interfaces*, 11 (2019) 40451.
53. S. Xu, Z. Lei, and P. Wu, *Journal of Materials Chemistry* A, 3 (2015) 16337.
54. X. Zhang, F. Meng, S. Mao, Q. Ding, M.J. Shearer, M.S. Faber, J. Chen, R.J. Hamers, and S. Jin, *Energy & Environmental Science*, 8 (2015) 862.
55. Q. Jia, C. Yu, W. Liu, G. Zheng, C. Lei, L. Lei, and X. Zhang, *Journal of Energy Chemistry*, 30 (2019) 101.
56. Z.M. Luo, J.W. Wang, J.B. Tan, Z.M. Zhang, and T.B. Lu, *ACS Applied Materials & Interfaces*, 10 (2018) 8231.
57. L. Liao, J. Sun, D. Li, F. Yu, Y. Zhu, Y. Yang, J. Wang, W. Zhou, D. Tang, S. Chen, and H. Zhou, *Small,* 16 (2020) 1906629.
58. J. Jadwiszczak, C. O'Callaghan, Y. Zhou, D.S. Fox, E. Weitz, D. Keane, C.P. Cullen, I. O'Reilly, C. Downing, and A. Shmeliov, *Science Advances*, 4 (2018) 5031.
59. Lin, He, Yang, Shihe, Hu, Jue, Long, Xia, Zhang, and Chengxu, *Journal of Materials Chemistry* A, 2017 (2017) 5995.
60. H. Zhou, F. Yu, Y. Huang, J. Sun, Z. Zhu, R.J. Nielsen, R. He, J. Bao, W.A. Goddard, III, S. Chen, and Z. Ren, *Nature Communications*, 7 (2016) 12765.
61. H. Wang, D. Kong, P. Johanes, J.J. Cha, G. Zheng, K. Yan, N. Liu, and Y. Cui, *Nano Letters*, 13 (2013) 3426.
62. Q. Gong, L. Cheng, C. Liu, M. Zhang, Q. Feng, H. Ye, M. Zeng, L. Xie, Z. Liu, and Y. Li, *ACS Catalysis*, 5 (2015) 2213.
63. X.-X. Ma, X.-H. Dai, and X.-Q. He, *ACS Sustainable Chemistry & Engineering*, 5 (2017) 9848.
64. B. Chakraborty, S. Kalra, R. Beltran-Suito, C. Das, T. Hellmann, P.W. Menezes, and M. Driess, *Chemistry - An Asian Journal*, 15 (2020) 852.
65. T. Singh, C. Das, N. Bothra, N. Sikdar, S. Das, S.K. Pati, and T.K. Maji, *Inorganic Chemistry*, 59 (2020) 3160.
66. R.Q. Yao, H. Shi, W.B. Wan, Z. Wen, X.Y. Lang, and Q. Jiang, *Advanced Materials*, 32 (2020) 1907214.
67. Q. Zhang, Z. Haixia, F. Meng, D. Bao, X. Zhang, and X. Wei, *Nano Research*, 11 (2018) 1294.
68. R. Hao, Y. Fan, T.J. Anderson, and B. Zhang, *Analytical Chemistry*, 92 (2020) 3682.
69. J. Zheng, W. Zhou, T. Liu, S. Liu, C. Wang, and L. Guo, *Nanoscale*, 9 (2017) 4409.
70. K. Liu, F. Wang, T.A. Shifa, Z. Wang, K. Xu, Y. Zhang, Z. Cheng, X. Zhan, and J. He, *Nanoscale*, 9 (2017) 3995.
71. L. Fang, W. Li, Y. Guan, Y. Feng, H. Zhang, S. Wang, and Y. Wang, *Advanced Functional Materials*, 27 (2017) 1701008.
72. X. Zhang, X. Cui, Y. Sun, K. Qi, Z. Jin, S. Wei, W. Li, L. Zhang, and W. Zheng, *ACS Applied Materials & Interfaces*, 10 (2017) 745